Gao WZ, Li CS, Xu CD, Wang D, Wu D.

An experimental investigation of salt-water separation in the vacuum flashing assisted with heat pipes and solid adsorption.

***Desalination* 2016, 399, 116-123.**

An experimental investigation of salt-water separation in the vacuum flashing assisted with heat pipes and solid adsorption

Wenzhong Gao[1],Changsong Li[1], Changda Xu[1], Dong Wang[1], Dawei Wu[2]

(1. Merchant Marine College, Shanghai Maritime University, Shanghai, 201306, China

(2. School of Marine Science and Technology, Newcastle University, Newcastle upon Tyne, NE1 7RU,United Kingdom)

Abstract

A novel single stage vacuum evaporator, as a salt-water separator, is developed to fully use ultra-low grade heat source as low as 50℃. The novel design incorporates several technologies, including heat pipes (HPs), spray flashing and solid adsorption. Its performance is evaluated by separating water from NaCl solution with 3%concentration. The results of the experiment study show that HPs transfer heat to the droplets rapidly to assist a second evaporation and maintain the superheat degree for the salt-water separation process after the flash evaporation. It is also found that, when the adsorbent beds are applied, the evaporation pressure decreases by 0.4-1kPa compared to the early experiment results, which results in an increase of the superheat degree. The introduction of solid adsorption in the salt-water separator provides a new way to utilize ultra-low grade heat source, although it brings a mixed success to the whole device while the separation ratio is slightly lower than expected due to the fact that there are both improved and impaired effects of heat transfer during the whole adsorption process. The lower cooling water temperature of the adsorption process, leads to better desorption effect, which improves the overall performance of the salt-water separator.

Keywords: Salt-water separation; Heat pipe; Solid adsorption; Vacuum evaporator

Nomenclature

HP	heat pipe	T	heat source temperature (℃)
m	condensed water mass (kg)	T_c	cooling water temperature (℃)
P	heat pipe average power (W)	T_{hp}	heat pipe surface temperature (℃)

P_s	evaporator pressure (kPa)	T_s	initial superheat degree (℃)
P_l	condenser pressure (kPa)	T_x	adsorbent bed temperature (℃)
t	elapsed time (s)	η	water separation ratio (%)

1. Introduction

Separating salts from seawater can be realized via evaporation and concentration, cooling crystallization, reverse osmosis technologies, etc. These technologies have been applied in many areas including desalination, liquid desiccant, and sewage disposal [1-4]. However, due to the existing technology constrains, the driving heat source temperature for these technologies normally exceeds 100□, i.e. the water boiling temperature. Double-effect lithium bromide absorption air conditioning, for example, needs driving heat source temperature over 130 ℃. Ultra-low grade heat in the temperature range of 40-100□, which is abundant from renewable energy and waste heat sources, has not been effectively utilized [5]. Therefore, exploring efficient methods of salt-water separation which uses ultra-low grade heat becomes increasingly appealing from a sustainable perspective.

As the core component of vacuum flashing salt-water separation device, vacuum evaporator has become a research focus in recent years. Dan Zhang [6] investigated static flash evaporation of NaCl solution when the superheat degree was between 1.7-53.9 K. It was reported that vapor quality is improved with the increasing initial solution height, while the vapor production per unit mass of NaCI solution decreased, because the increasing static pressure of bottom liquid restrains the flash process. Besides, it was also found that vapor quality is increased linearly with increasing the superheat degree. Furthermore, through adopting the spray flash evaporation method proposed by O.Miyatake et.al [7-8], A. Günther [9] and Sami Mutai [10] injected atomized liquid spray into the low pressure environment to accelerate the flashing process. The interaction between the flash and liquid atomization was studied, which indicates that flash intensifies the atomization effect and reduces droplets' size even when the superheat degree was relatively small. Consequently, the flash evaporation rate and ratio are improved and the non-equilibrium temperature difference is reduced. However, the researchers [9, 10] focused on improving the conversion rate from sensible heat to latent heat, rather than enhancing the separation ratio fundamentally. Therefore, the single stage separation ratio is only 0.8-1.4%ofthe traditional vacuum flash desalination devices.

In order to discover the relationship between heat and temperature variations in the flash process of

droplets, C.M. Augusto [11] and Wenlong Chenget.al. [12] conducted the researches on the formation and the temperature variations of the droplets during the vacuum flashing. The results showed that, during the static flash evaporation, the droplets' final temperature is decreased when the pressure gets lower or the droplets become smaller. It is reported that it takes more time to reach the lowest temperature when droplets' original temperature is high. Other researchers [1, 2] studied the temperature distribution of lithium chloride droplets during the vacuum flashing process. It was found that the radiant heat significantly promotes the flash evaporation. Therefore, the heat supply in a timely manner to the flash evaporation is the critical requirement for maintaining the evaporation intensity. In terms of that, heat pipes (HPs) can be used as an ideal media in the heat transfer process due to their high heat transfer coefficient even better than the heat conductivity of metals. Xuehua Guo [13] and Qian Yang [14] applied the gravity HPs into single stage vacuum evaporators. Heat within engine jacket water is absorbed by HPs, and then transferred to seawater, which forms a falling film on the HP's cold side surface. Because the solution absorbs heat continuously during the falling process, the superheating is well maintained. It is mentioned that the single stage separation ratio reached up to 8-30% [13, 14].In other literatures, H. Jafari Mosleh[4] applied HPs to a novel solar-driven desalination device, which achieved fresh water yield of 0.933 $kg \cdot m^{-2} \cdot h^{-1}$ and improved the utilization ratiofrom22.5% to 65.2%.

In order to maintain the low pressure during the flash evaporation, steam generated in the evaporator must be transferred into liquid form quickly. Compared to the traditional direct condensation using cooling water, solid adsorption technology can dramatically reduce the steam pressure to a lower level in the system. Its potential in desalination has attracted wide attention in recent years. National University of Singapore made some remarkable achievements on the application of solid adsorption in desalination [15-18]. Solid adsorbent was introduced into the process to replace the traditional condensing system, which lowers the evaporation temperature to 4-5℃.Based on that, they remarkably reduced the condensing pressure and increased the stage number of MED (Multi-effect Distillation) to achieve 1.5-2 times of the water producing ratio.

To incorporate the merits of the abovementioned technologies to fully utilize ultra-low grade heat and strengthen the evaporation intensity, the authors [19] developed a novel vacuum evaporator, which includes two separation processes: the spray flash prime evaporation and the second evaporation reheated by the HPs and assisted by the solid adsorption. The water separation process and the fresh water yield per unit

volume are improved greatly. When solid adsorbent beds were added into the system, the vacuum pressure was maintained at a very low level, and eventually the vapor generated in the evaporator was absorbed by the adsorbent beds quickly. In this paper, a series of water separation experiments of NaCl solution with 3% salinity are reported, which identifies the heat and mass transfer characteristics, when the HPs and the adsorbent beds are adopted and integrated into the novel single stage vacuum evaporator for salt-water separation.

2. System description and working principle

2.1 Experimental rig setup

The experimental rig mainly consists of an evaporator, two adsorbent chambers, a condenser, a water circulation loop and two vapor channels. A schematic diagram of the setup is shown in Fig.1 and the picture of the rig is seen in Fig.2.

The evaporator is mainly composed of two blind plates and a toughened glass tube in between, the toughened glass tube is with the dimensions of inner diameter D= 135 mm, height H=450 mm as well as HPs with the dimensions of external diameter D=10 mm, wall thickness T= 0.5 mm, length L= 400 mm. Because of the cylindrical spray region, the HPs are plugged through the holes on the blind plate in a regular hexagon form including one drainage hole as shown in Fig.3.Sintered water-copper HPs, water as working fluid, are adopted in the experiment. The metal powder-sintering method is implemented in the internal wall of the HPs, resulting in strong hydrophilic and hydrophobic characteristics at the hot end and cold end respectively, which helps to improve the heat transfer performance significantly [20]. The HP performance parameters and thermocouple arrangement on the HPs are shown in Table 1 and Fig.4 respectively. A centrifugal nozzle head with the aperture of 0.3 mm used in the experiments can generate micro droplets with the diameters of 5-10 um under a pressure between 20-70 bars.

The adsorbent bed is made up of five sets of U-shaped aluminum finned stainless steel-made tube in each adsorbent chamber. 8 kg of ‘Type A’ fine pored silica gel with the diameters of 0.5-1.5 mm is packed between the fins by the wire mesh. Thermocouple arrangement on the adsorbent bed is shown in Fig.5. There are 8magnetic valves in the water circuits to switch hot water and cold water pathways.

T thermocouples with the precision of ±0.5 ℃ are used for temperature measurement. Pressure gages with range of 0-20 kPa and accuracy of 0.1% are set in the evaporator and condenser. Because the adsorbent chamber has a large flow area and it is close to the evaporator and condenser, the measured value

of pressure also stands for the adsorbent chamber pressure.

The working principle of the experimental setup is as follows. The high pressure in the centrifugal nozzle atomizes the preheated solution into micro droplets and sprays them into the vacuum evaporator. After two separation process including the spray flash evaporation and the HP reheating second evaporation, steam is transferred to the adsorbent bed 'A' through adsorption. The remaining concentrated solution is pumped out. Adsorbent bed B is heated by hot water at the same time, and the vapor desorbed will condensation in condenser. The adsorbent bed 'A' and 'B' is set to perform desorption or adsorption alternatively by switching the valves, ensuring the continuity of the experiment [21].The temperature and pressure of both adsorption and desorption process will change with the heat and mass transfer process.According to the mass balance, the mass of adsorption is equal to the mass of desorption and the mass of condensed water in one operation cycle.

2.2 Experiment parameters

The experiment examines the influence of the adsorbent beds and HPs in the heat and mass transfer process. The main parameters involved are the water temperature T in the heating tank1, the cooling water temperature T_c in the cooling tank, the water separation ratio η, the heat pipe surface temperature T_{hp} and the heat pipe average power P. The water separation ratio η is defined as the ratio of condensed water mass and the dilute solution mass. The volume of the solution is measured by liquidometer and the mass of solution is calculated through the volume and density. The HPs' average power is calculated by the heat balance. Experimental Conditions are shown in Table 2. The spray flow-rate is 120 $ml \cdot min^{-1}$ and the spray temperature is 50 ℃. Temperature of hot water in heating tank 2# for desorption is 90 ℃. The data is collected in the half-cycle time which is set at 1800 s.

3. Results and discussion

3.1 HP's surface temperature distribution and heating power

In order to obtain accurate temperature distribution of the HPs' surface, the thermocouples are mounted at ten locations. Fig.6 shows the average temperature of each of the equidistant position, and the average power of the HPs is shown in Fig.7. The results indicated that, under the same conditions, the temperature differences of five measuring points at the hot side are small, and so did the temperature differences on the cold side. The overheated droplets flashed as a result of instantaneous depressurization and resulted in a rapid temperature drop of its main body. Lowest temperature appeared in1# measuring point because it was

the nearest point to the flashing droplets. Thus the measured values are influenced by both the HP's surface and the flashing droplets, even though insulating materials has been taken to reduce the impact of the flashing droplets. Also, the temperature measuring point5#was immersed in the base of the evaporator and its temperature was inevitably influenced by the concentrated solution. Hence the measured value was also lower than the real HP's surface value.

The temperature difference between the hot and the cold sides of the HPs as well as its surface temperature become increasingly large when the heat source temperature rises. The values of the same temperature measuring point decreases lightly and HP's average power increases marginally when the cooling water temperature gets lower. This is because the lower cooling water temperature decreases the adsorbent bed temperature, enabling strengthens adsorption driving forces. Thus the evaporator pressure reduces, leading to lower droplet temperatures after flash evaporation. These indicate that the heat source temperature is the main influence factor of HP's surface temperature and its average power. It must be pointed out that because of the application of the adsorbent bed, the evaporator pressure reduces significantly at the preliminary stage of adsorption, which is why the temperature value at the same measuring point are generally lower than that of without the adsorbent beds[19], while the temperature difference of the both ends of HP increases by 2-3 ℃. Besides, the dotted line of Tc'=25 ℃ in Fig.7 represents the HP's average power curve under the cooling water temperature is 25 ℃, when the evaporator is connected to the condenser directly without the adsorbent bed . It is obvious that the average power of HP is higher than that of with adsorption bed. The above results indicate that adopting adsorbent has both improved and impaired effects on heat and mass transfer during the adsorption process.

The temperature difference between the hot end and cold ends of the HPs is 13-21℃, while the corresponding HP's power is 36-126 W. The outer surface temperature of the heat pipe is mainly affected by the pressure and intensity of the droplets' flash. Therefore, the conclusion can be made that the HP's power increased significantly with the increase of the temperature difference of the two ends of the HPs. This matches the conclusion made by C Ferrandi [22] and B Ch Nookaraju[23]. The former conducted their experiments by using a sintered copper HP with the length of 1 m and gained power of 132 W when the temperature difference was 20 ℃. B Ch Nookaraju's corresponding data were 565 mm, 100 W and 40 ℃.

3.2 Evaporator pressure

Pressure changes in the evaporator of six conditions are shown in Fig.8. The figure indicates that the evaporator pressure reduces sharply at first and then rises slowly. The reason is supported by the fact that the adsorption rate is much stronger in the initial phase. As a result, the adsorption rate is much faster than the steam generation rate, leading to a significant reduction of the evaporator pressure. Simultaneously, the steam saturation temperature also decreased. It indicates that, under the same spray temperature, the increase of droplets' superheat degree results in the enhanced flash intensity and lower droplet temperature after the flash evaporation. Therefore, the cold end temperature of the HP decreased and the temperature difference of the two ends increased. However, in the next stage when adsorbent gradually saturated and the steam generation rate exceeded its absorption rate, the evaporator pressure began to rises slowly. In order to ensure its adsorption capacity, the adsorbent beds should be switched alternatively to start the second half of a cycle when one bed reaches its saturated adsorption capacity.

Besides, it can be found inFig.8 that under the same cooling water temperature, the evaporator pressure grows along with the heat source temperature. Similarly, under the same heat source temperature, the lower cooling water temperature is, the lower evaporator pressure will be. However, the evaporator pressure difference is not very obvious when changing cooling temperature from 25℃ to 15℃, except when the heat source temperature raised to 90 ℃ and the evaporating pressure difference is approximately 1kPa. These trends indicate that the cooling water temperature has limited influence on the evaporation intensity when the heat source temperature is relatively low. On the contrary, the heat source temperature is the key factor of the pressure dynamic balance in the evaporator.

Fig.9 shows the pressure comparisons with the adsorbent beds and without the adsorbent beds under the same other operate parameters. C4'represents the condition that has no adsorbent beds, and the data are derived from our previous experiments [19]. As shown, with the adsorbent beds, the evaporator pressure lowers by 0.4-1kPa for about 500 s than that of without the adsorbent beds. Therefore, in order to take advantage of adsorbent on using ultra low grade heat source, switching time of two adsorbent beds is preferably less than 500 seconds.

3.3 Adsorbent bed temperature in the adsorption process

Fig.10 illustrates the temperature change of the adsorbent beds versus time during the adsorption process. The figure indicates that the average temperature of the adsorbent bed rises rapidly in the beginning and then declines gradually after a peak when the heat source temperature is 70℃ or 90℃.On the other hand,

the change of average temperature is far less obvious under the heat source temperature of 50℃. The reason is that the adsorbent bed that just being desorbed has strong affinity to water vapor at the initial stage of adsorption. Hence a large amount of vapor is absorbed, releasing massive adsorption heat which is beyond the cooling power. Thus adsorbent bed temperature rises greatly. With the increase of adsorption uptake, the adsorption rate decreases gradually, so does the adsorption heat. Moreover, the droplet evaporation intensity is weak as well as the generation rate of steam when the heat source temperature is 50℃, so the adsorbent bed can be cooled in time by the cooling water. As a result, the average temperature of the adsorbent bed is relatively stable.

3.4 Condenser pressure

Pressure changes in the condenser are shown in Fig. 11.It can be seen that the pressure falls rapidly at first and then tend to be flat. The final pressure values are almost the same for different conditions but with the same cooling water temperature. This is because in the initial stage of desorption, the partial pressure of steam in the adsorbent bed is much higher than it is on the condenser coil surface. Thus the driving pressure of condensation is pretty strong promoting condensation and causing a remarkable drop of condenser pressure. As the adsorbent temperature rises, the partial pressure of steam on the adsorbent surface keeps reducing gradually, so does the driving pressure of condensation until the equilibrium is established between the partial pressure of steam and the condenser pressure. Indeed, the final equilibrium pressure in the condenser is determined by the cooling water temperature.

Furthermore, it is noticed from different angle that the initial pressure in the condenser rises along with the heat source temperature. The condenser pressure in all of the conditions drops sharply at the beginning of the desorption process and takes longer time to become stable. The reason is that increasing heat source temperature can increase adsorption quantity and raise the final evaporator pressure. Large amount of steam is condensed quickly at the beginning of desorption process, causing a fast drop of the condenser pressure. However, larger adsorption quantity gives rise to longer desorption time as well as the certain condenser capacity. Although different heat source temperatures result in a remarkable difference of the adsorbent bed pressures at the beginning of desorption process, it has limited influence on the rate of desorption and equilibrium pressure which are mainly decided by the cooling water temperature. Hence, when given the same desorption temperature, the lower cooling water temperature leads to better desorption effect.

3.5Adsorbent bed temperature in the desorption process and adsorption quantity

When the adsorbent bed is saturated, it will be switched to the mode of desorption, and hot water flows within hot water tubes through the adsorbent bed. The temperature of hot water in tank 2# was 90℃ and stable in our experiments. Fig.12.shows the temperature changes in the adsorbent bed during the desorption process. It can be found from the curves that adsorbent bed temperature decreases slightly at first and then keeps stable for a short time before raising sharply at last. The reason for the slight decrease is that the adsorbent bed contains a large amount of water just after switching from adsorption to desorption. Therefore, the desorption is in its highest rate at the beginning under the same driving pressure by cooling water mentioned above, which can also be proved by the slope of the mass of condensate water shown in Fig.13. The heat provided by hot water is not able to offset the required desorption heat during this period. As a result, the adsorbent bed temperature shows a slight decline. With the process of desorption, the rate of desorption reduces and the heat provided by the hot water gradually surpasses the desorption heat. Therefore, the water vapor pressure difference between the adsorbent surface and the condenser decreases gradually, which can be proved by the raising adsorbent bed temperature after its initial stationary phase.

On the other hand, when the heat source temperature is only about 50 ℃ of both Condition1 and Condition2,adsorption quantity and driving pressure difference are small as well as desorption heat. The adsorbent bed temperature barely decreases and increases sharply after 400s. Also when heat source temperature rises to 90℃ in Condition5 and Condition6,the adsorbent bed temperature reduces more sharply at the beginning then stays stable for 1000s.It illustrates that, by increasing heat source temperature, the time of high desorption rate can be obviously extended and more condensed water can be obtained.

In brief, the above phenomena indicate that low heat source temperature leads to small adsorption quantity even if the adsorbent bed lowers the evaporator pressure and uses lower grade energy. Therefore, more adsorbent needs to be added to gain the same water separation ratio that achieved with high heat source temperature. Also, cooling capacity has impact on not only the mass of condensed water but also desorption time. To achieve better match between adsorption and desorption, it is recommended to adjust the cooling water amount dynamically in the adsorbent bed during adsorption process and the cooling power for the

condensing coil during the desorption process.

3.6Water separation ratio

Accumulated water mass separated from the solution under different cooling temperatures are shown in Fig.13. When the rest of parameters are fixed, the higher heat source temperature and the lower cooling water temperature leads to the higher separation ratio. Because the higher heat source temperature can enhance the superheat degree and evaporation intensity when the droplets come into contact with the cold side of the HPs. Furthermore, both the evaporation capacity and adsorption quantity increase at the same time and the temperature difference of two sides of the HPs becomes bigger. On the other hand, the lower cooling water temperature results in the decrease of the adsorbent bed temperature as well as the steam partial pressure on the sorbent surface. Thus, the adsorption quantity increases slightly alongside the driving pressure difference. The dotted line of Tc'=25 ℃in Fig.14represent the separation ratio curve at the same temperature when the evaporator is connected to the condenser directly. As the HP's average power reflects the heat acquired by the solution, similarly the curve values indirectly determines the mass of condensed water and the separation ratio. It should be pointed out that the decrease of the separation ratio after the application of the adsorbent beds could be explained by the same reasons as the HP's average power above. Therefore, the heat source temperature is the core factor of the fixed adsorbent bed that influences the salt-water separation ratio greatly.

4. Conclusions

In order to improve the single-stage water separation ratio, a novel design is proposed in this paper, in which the HPs transfer the heat to droplets for a second evaporation after the initial spray flash evaporation, and the adsorbent beds absorbs steam generated in the evaporator quickly to maintain the vacuum level. Compared to traditional single-stage flash evaporator, the new design decreases the evaporation pressure, in turn, increases the water separation ratio from 5%to 46%, which allows a more compact device driven by ultra-low grade heat source from minimum temperature of 50 °C. Main conclusions of the present work are drawn as follows:

(1) Heat source temperature is the core factor of the salt-water separation. The HP's cold side temperature and power, the thermal energy acquired by the droplets, and the evaporation intensity all increase with the growth of the heat source temperature. Decreasing cooling water temperature has limited influence on the evaporation intensity when the heat source temperature is relatively low. The heat source

temperature is also the key factor of the equilibrium pressure in the evaporator.

(2)A stage, obtaining 0.4-1kPalowerevaporator pressure by using adsorbent, is gained, resulting in the improvement of droplets' superheat degree. However, in order to take advantage of adsorbent, switching time of two adsorbent beds is preferably less than 500 seconds. Simultaneously, it is crucial to transfer adsorption heat quickly.

(3) Adopting adsorbent bed provides a new way to utilize lower grade heat source in salt-water separation. Nevertheless, enough adsorbent is needed to obtain the same water separation ratio because low heat source temperature shrinks adsorption quantity.

(4) Different heat source temperature causes remarkable difference of the adsorbent bed pressures at the beginning of the desorption process. However, it has limited influence onthe desorption time and the equilibrium pressure. Both parameters are effectively determined by the cooling water temperature because the lower cooling water temperature means higher desorption rate.

Acknowledgments

The research work described in this paper was supported by the National Natural Science Foundation of China (Grant No.51106094)as well as Natural Science Foundation of Shanghai (Grant No. 16ZR1414700). Their supports are gratefully acknowledged by the research team.

Reference

[1] W.Z. Gao, W.Z. Sun, Keith Anderson, Y.P. Cheng, Ang Li. Investigation on temperature distribution of flash evaporation of LiCl droplets released into vacuum. International Journal of Heat and Mass Transfer 74 (2014) 414-420.

[2] W.Z. Gao, Y.Z. Shi, X.L. Zhang, Keith Anderson. Experimental investigation on a new method of regenerating dehumidification solution–release solution droplet into vacuum. Applied Thermal Engineering 59 (2013) 14-20.

[3] Yunan Wang. Experimental Study of Multi-effect Distillation Oilfield Wastewater Desalination System. Dalian University of Technology. 2014.

[4] H. JafariMosleh, S. JahangiriMamouri, M.B. Shafii, A. Hakim Sima. A new desalination system using a combination of heat pipe, evacuated tube and parabolic trough collector. Energy Conversion and Management 99 (2015) 141-150.

[5] Haiyan Li, Jing Liu. Current Research Status, Difficulties and New Strategy in Utilization of Low

Grade Heat. Science & Technology Review 17 (2010) 112-117.

[6] Dan Zhang, Daotong Chong, Junjie Yan, Bingchao Zhao. Experimental study on static flash evaporation of aqueous NaCl solution. International Journal of Heat and Mass Transfer 55 (2012) 7199-7206.

[7] O. Miyatake, T. Tomimura, Y. Ide, T. Fujii. An experimental study of spray flash evaporation. Desalination 36 (2) (1981) 113-128.

[8] O. Miyatake, T. Tomimura, Y. Ide, M. Yuda, T. Fujii. Effect of liquid temperature on spray flash evaporation. Desalination 37 (3) (1981) 351-366.

[9] A. Günther, K.-E. Wirth. Evaporation phenomena in superheated atomization and its impact on the generated spray.□International Journal of Heat and Mass Transfer 64 (2013) 952-965.

[10] Sami Mutair, Yasuyuki Ikegami. Experimental investigation on the characteristics of flash evaporation from superheated water jets for desalination. Desalination 251 (2010) 103-111.

[11] C.M. Augusto, J.B. Ribeiro, A.R. Gaspar, J.J. Costa. Low-pressure-vaporization of free water-Characterization of the boiling regimes. International Journal of Thermal Sciences 77 (2014) 19-26.

[12] Wenlong Cheng, Lei Hu, Hua Chen, Weiwei Zhang, Biao Xie. Influence of Characteristics of Non-Isothermal Flashing Droplet on Vacuum Flash-Spray Cooling.□Chinese Journal of Vacuum Science and Technology 4 (2015) 399-404.

[13] Xuehua Guo. Design and experimental study of heat-pipe vacuum evaporator. Dalian University of Technology. 2000.

[14] Xi Yang. Research and development of heat pipe desalination plant. Qingdao University of Science and Technology. 2014.

[15] Kim Choon Ng, Kyaw Thu, Youngdeuk Kim, Anutosh Chakraborty, Gary Amy. Adsorption desalination: An emerging low-cost thermal desalination method. Desalination 308 (2013) 161-179.

[16] A. Li, A. B. Ismail, K. Thu, M. W. Shahzad, K. C. Ng, B. B. Saha. Formulation of water equilibrium uptakes on silica gel and ferroaluminophosphate zeolite for adsorption cooling and desalination applications. Evergreen 01 (02) (2014) 37-45.

[17] A. Li, K. Thu, A. B. Ismail, M. W. Shahzad, K. C. Ng. Performance of adsorbent-embedded heat exchangers using binder-coating method. International Journal of Heat and Mass Transfer 92 (2016) 149-157.

[18] Kim Choon Ng, Kyaw Thu, SeungJin Oh, Li Ang, Muhammad Wakil Shahzad, Azhar Bin Ismail.

Recent developments in thermally-driven seawater desalination: Energy efficiency improvement by hybridization of the MED and AD cycles. Desalination 356 (2015) 255-270.

[19] Wenzhong Gao，Changsong Li, Changda Xu, Dong Wang. Experimental study on water separation process in a novel spray flash vacuum evaporator with heat-pipe. Desalination 386 (2016) 39-47.

[20] M Rahimi, K Asgary, S Jesri. Thermal characteristics of a resurfaced condenser and evaporator closed two-phase thermo syphon. International Communications in Heat and Mass Transfer 37 (6) (2010) 703-710.

[21]Ya-Song Sun, Jing Ma, Ben-Wen Li, Zhi-Xiong Guo. Prediction of nonlinear heat transfer in a convective-radiative fin with temperature dependent properties by the collocation spectral method. Numerical Heat Transfer Part B, 2016, 69(1): 63-68.

[22] C Ferrandi, F Iorizzo, M Mameli, S. Zinna, M. Marengo. Lumped parameter model of sintered heat pipe: Transient numerical analysis and validation. Applied Thermal Engineering 50 (2013) 1280-1290.

[23] B. ChNookaraju, P.S.V. KurmaRao, S. Naga Sarada. Thermal Analysis of Gravity Effected Sintered Wick Heat Pipe. Materials Today: Proceedings 2 (2015) 2179-2187.

Table 1 Performance index of the HPs

Performance index	Range	Units
Operating temperature	0～200	℃
Fail temperature	340	℃
Working life at 80℃	>7	Year
Rated power	100	W
Fluid media	water	/

Table 2 Experiments under different input conditions

Condition	Heat source temperature/℃ (heating tank1#)	Cooling temperature/℃ (cooling tank)
1	50	15
2	50	25
3	70	15
4	70	25
5	90	15
6	90	25

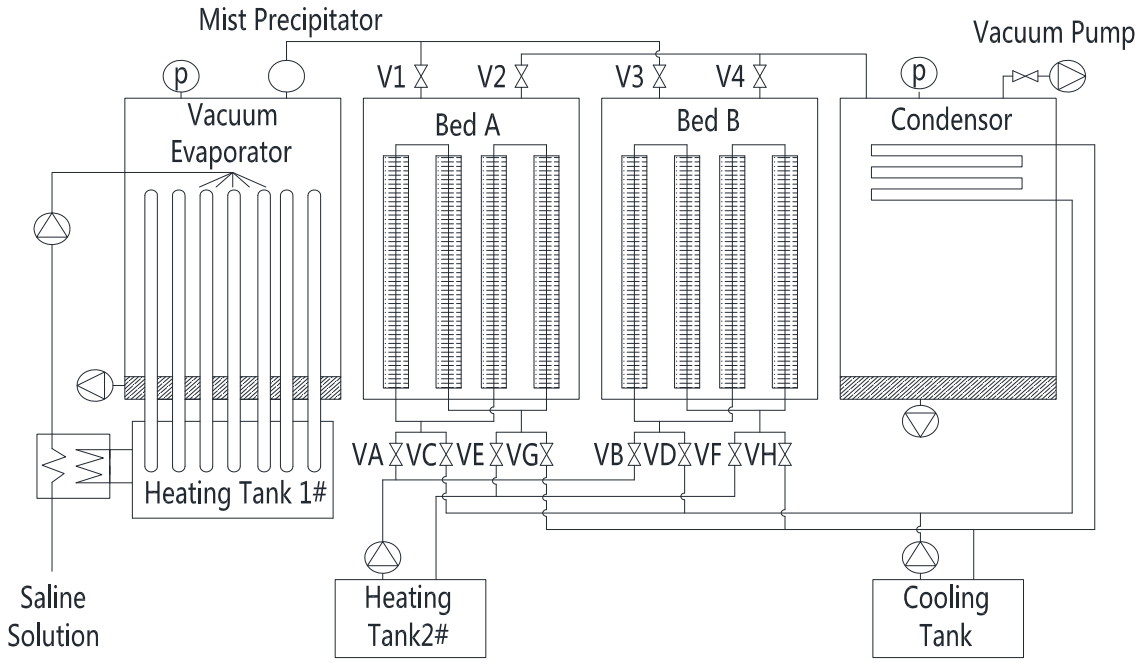

Fig.1 Schematic diagram of the experimental rig

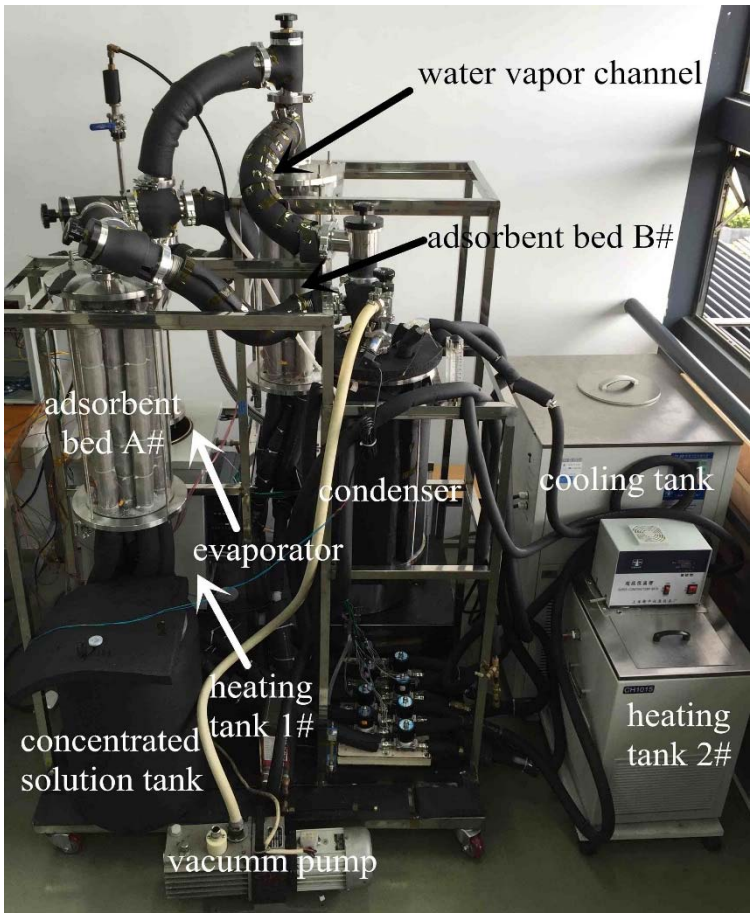

Fig.2 Photo of the experimental rig.

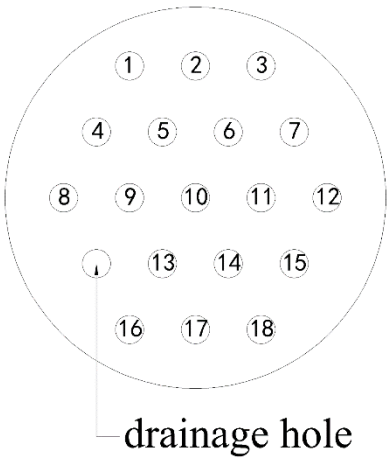

Fig.3 HPs distribution on the blind plate

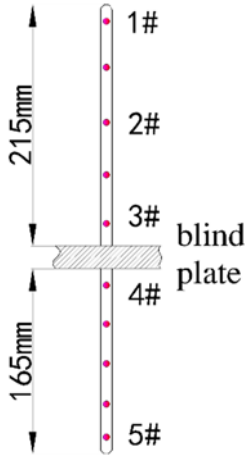

Fig.4 Thermocouple arrangement on the HP outer surface

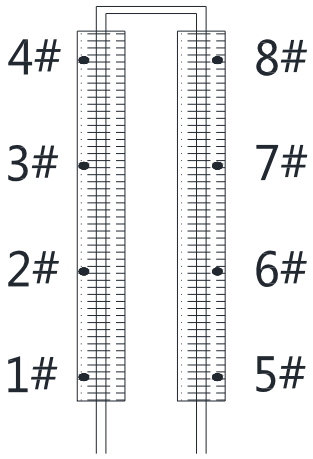

Fig.5 Thermocouple arrangement in the adsorbent bed

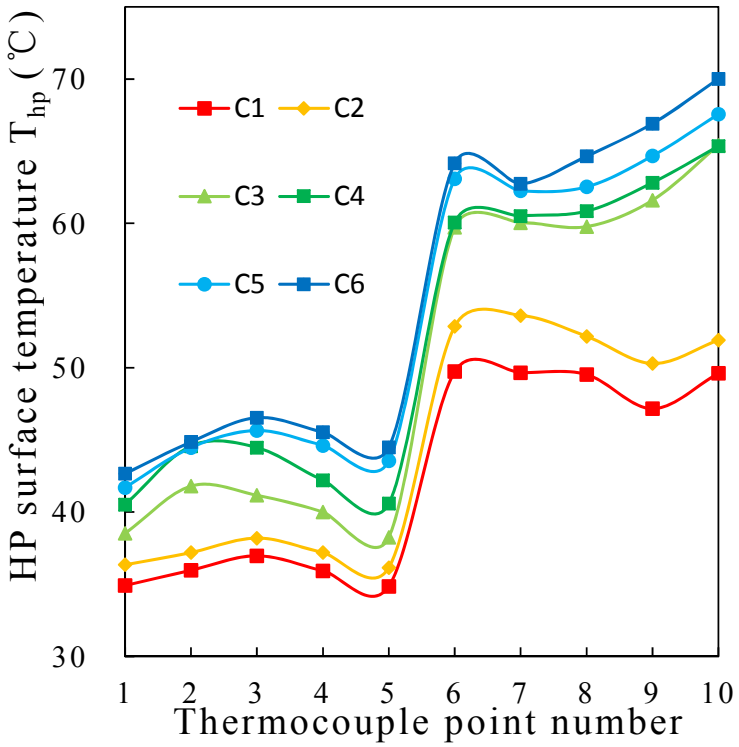

Fig.6 The HP surface temperature distribution

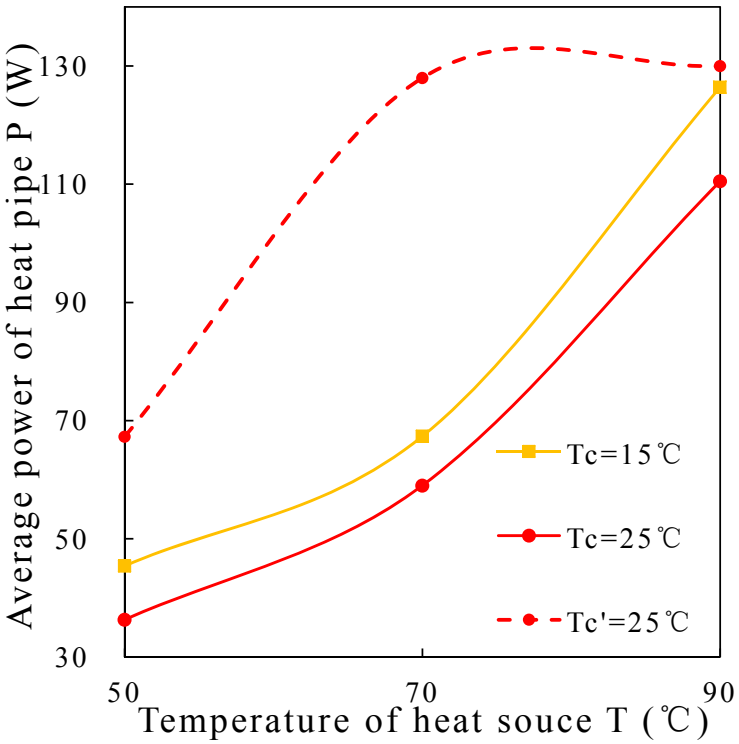

Fig.7 Heat pipe average power vs temperature

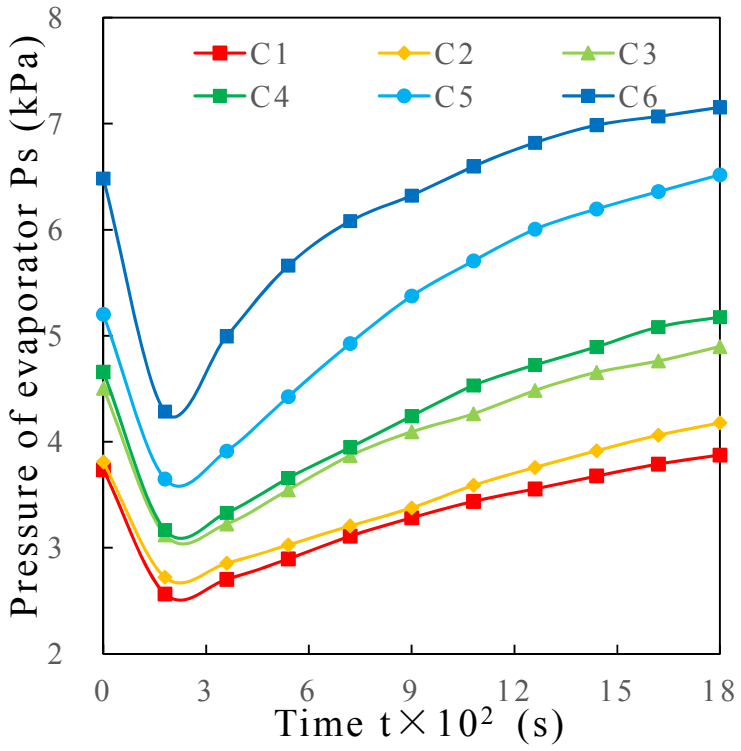

Fig.8 Evaporator pressure vs time

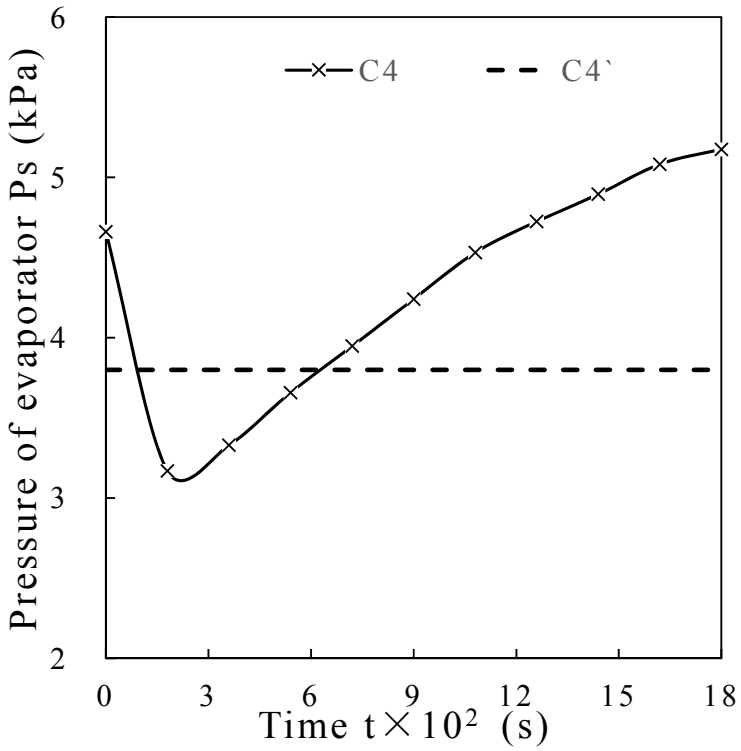

Fig.9 Pressure of evaporator vs time under C4 and C4'

(C4'repersents the condition that has no adsorbent beds)

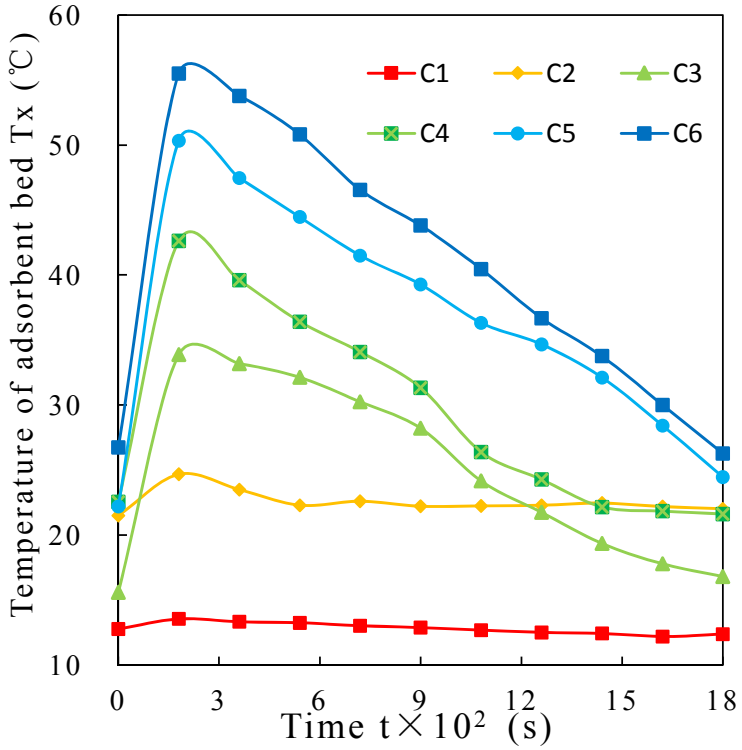

Fig.10 Temperature of the adsorbent bed vs. time during the adsorbing process

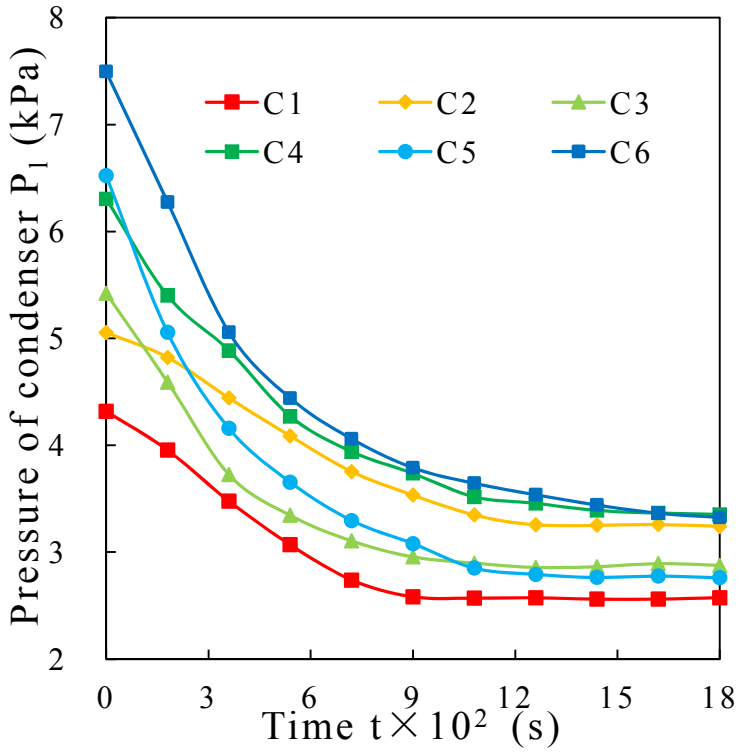

Fig.11 Pressure of the condenser vs. time

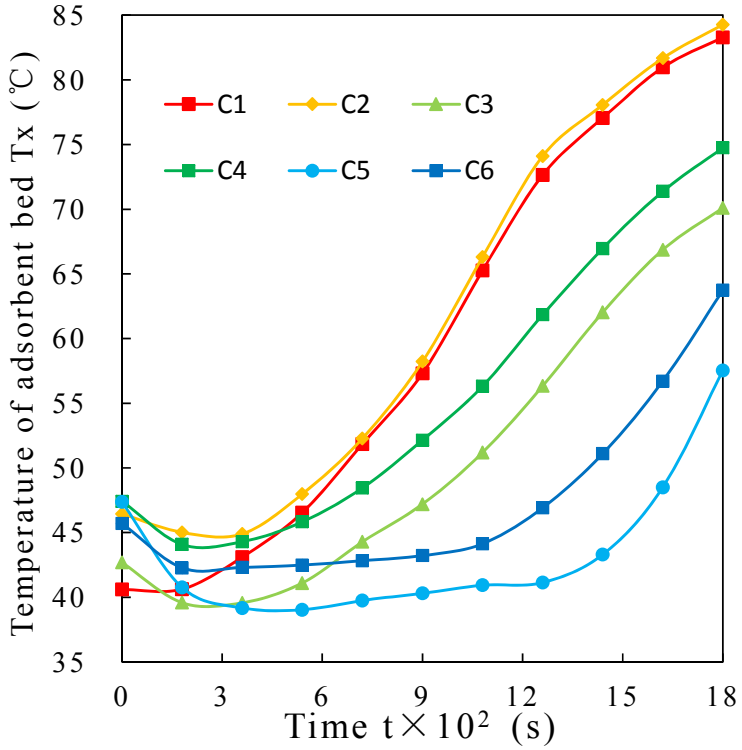

Fig.12 Temperature of the adsorbent bed vs. time during the desorbing process

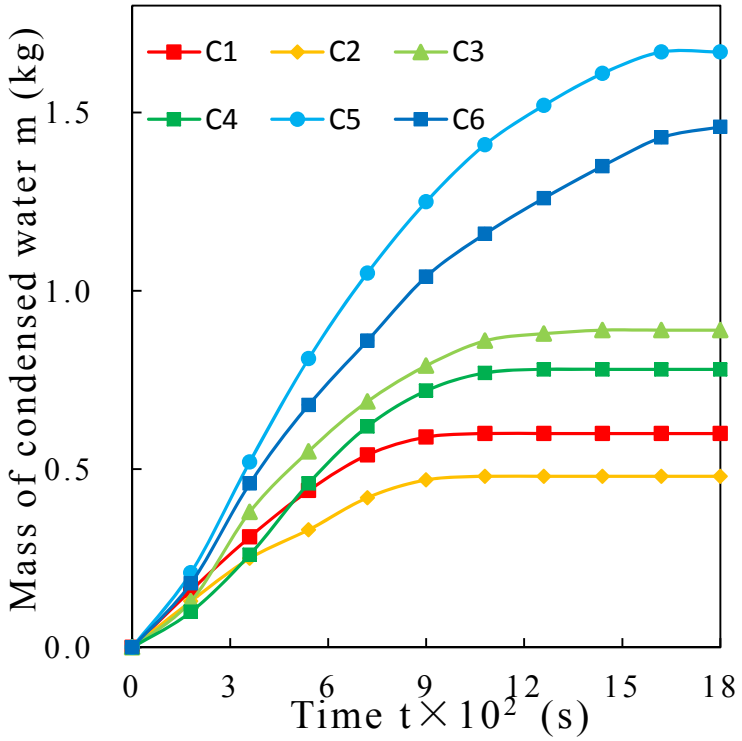

Fig.13 Mass of condensed water vs. time

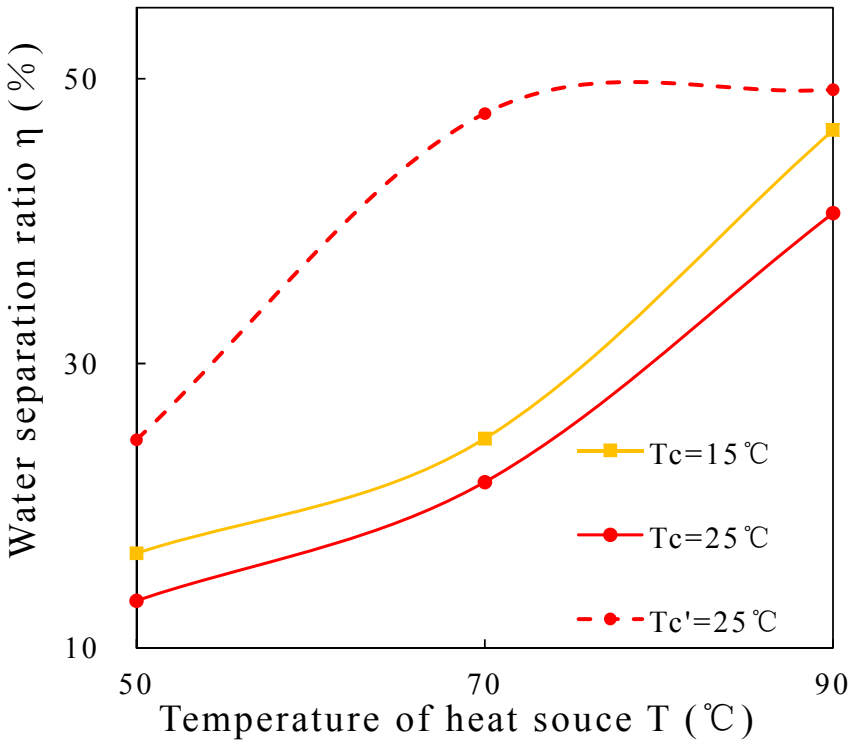

Fig.14 Separation rate with different cooling temperatures